BJC British Journal of Cancer

www.nature.com/bjc

ARTICLE

Translational Therapeutics

DNMTi/HDACi combined epigenetic targeted treatment induces reprogramming of myeloma cells in the direction of normal plasma cells

Angelique Bruyer[1], Ken Maes[2], Laurie Herviou[1], Alboukadel Kassambara[1,3], Anja Seckinger[4], Guillaume Cartron[5,6,7], Thierry Rème[1,3], Nicolas Robert[3], Guilhem Requirand[3], Stéphanie Boireau[3], Carsten Müller-Tidow[4], Jean-luc Veyrune[1,3], Laure Vincent[6], Salahedine Bouhya[6], Hartmut Goldschmidt[4,8], Karin Vanderkerken[2], Dirk Hose[4], Bernard Klein[1,3,5], Elke De Bruyne[2] and Jerome Moreaux[1,3,5]

BACKGROUND: Multiple myeloma (MM) is the second most common hematologic malignancy. Aberrant epigenetic modifications have been reported in MM and could be promising therapeutic targets. As response rates are overall limited but deep responses occur, it is important to identify those patients who could indeed benefit from epigenetic-targeted therapy.
METHODS: Since HDACi and DNMTi combination have potential therapeutic value in MM, we aimed to build a GEP-based score that could be useful to design future epigenetic-targeted combination trials. In addition, we investigated the changes in GEP upon HDACi/DNMTi treatment.
RESULTS: We report a new gene expression-based score to predict MM cell sensitivity to the combination of DNMTi/HDACi. A high Combo score in MM patients identified a group with a worse overall survival but a higher sensitivity of their MM cells to DNMTi/HDACi therapy compared to a low Combo score. In addition, treatment with DNMTi/HDACi downregulated IRF4 and MYC expression and appeared to induce a mature BMPC plasma cell gene expression profile in myeloma cell lines.
CONCLUSION: In conclusion, we developed a score for the prediction of primary MM cell sensitivity to DNMTi/HDACi and found that this combination could be beneficial in high-risk patients by targeting proliferation and inducing maturation.

British Journal of Cancer https://doi.org/10.1038/s41416-018-0025-x

INTRODUCTION

Multiple myeloma (MM) is a most often fatal neoplasia characterized by the accumulation of malignant plasma cells (MMCs) in the bone marrow (BM). The profile of DNA methylation in MM comprises genomic global hypomethylation and simultaneous promoter hypermethylation of known or potential tumor-suppressor genes[1, 2]. Recently, hypermethylation of several potential suppressor genes was demonstrated to be associated with significantly shorter overall survival (OS)[1].

Decitabine (5-aza-2′-deoxycytidine) and 5-azacytidine are both clinically used DNA methyltransferase (DNMT) inhibitors (DNMTi) for the treatment of myelodysplastic syndrome (MDS) and acute myelogenous leukemia (AML)[3]. In MM, clinical trials are ongoing with DNMTi as monotherapy or combined with lenalidomide or dexamethasone[4]. Histone deacetylases (HDACs) also represent promising molecular targets for the treatment of different cancers, including MM[5–15]. Romidepsin and Vorinostat (SAHA) are two HDAC inhibitors (HDACi) that have been approved by the Food and Drug Administration (FDA) for the treatment of cutaneous T-cell lymphoma[16] and several pan-HDACi are currently evaluated in clinical trials in MM[4, 14]. Combination of panobinostat/bortezomib/dexamethasone (PANORAMA) and of vorinostat/bortezomib (VANTAGE 088) have been tested in two large phase III clinical trials[17, 18]. Results from the VANTAGE 088 trial showed that the association of vorinostat and bortezomib significantly prolonged progression-free survival (PFS) in patients with relapsed or refractory MM[17]. For the PANORAMA trial, re-evaluation of the results recently showed a significant improvement of the PFS when the pan-HDACi panobinostat was combined with bortezomib and dexamethasone in a prespecified subgroup of patients previously exposed to with both bortezomib and an immunomodulatory agent (IMiD) with relapsed MM resulted in a significant PFS improvement. In addition, the overall response rate was also higher: 59 vs 41%. The FDA and European Medicines Agency pproved panobinostat only very recently in patients who have received at least two prior lines of therapy, including bortezomib and an IMiD[19–21]. However, this

[1]IGH, CNRS, Univ Montpellier, Montpellier, France; [2]Laboratory of Hematology and Immunology, Myeloma Center Brussels, Vrije Universiteit Brussel, Brussels, Belgium; [3]Department of Biological Haematology, CHU Montpellier, Montpellier, France; [4]Dept. of Internal Medicine V, University of Heidelberg, Heidelberg, Germany; [5]UFR de Médecine, Univ Montpellier, Montpellier, France; [6]Department of Clinical Hematology, CHU Montpellier, Montpellier, France; [7]Univ Montpellier, UMR CNRS 5235, Montpellier, France and [8]National Center of Tumor Diseases, University of Heidelberg, Heidelberg, Germany
Correspondence: Jerome Moreaux (jerome.moreaux@igh.cnrs.fr)
These authors share first authorship: Angelique Bruyer, Ken Maes.
These authors contributed equally: Elke De Bruyne, Jerome Moreaux.

Received: 7 August 2017 Revised: 10 January 2018 Accepted: 15 January 2018
Published online: 02 March 2018

Published by Springer Nature on behalf of Cancer Research UK

Table 1. Pathway enrichment analysis using Reactome of genes significantly overexpressed in decitabine/TSA-treated HMCLs

Gene set name	k/K	# Genes in Gene Set (K)	# Genes in Overlap (k)	*P*-value	FDR *q*-value	Genes
Interferon alpha/beta signaling (R)	0.0069	67	18	0.0000	5.98E-13	IFITM1, IFITM2, IFIT1, IFIT3, IFIT2, RSAD2, IFI27, EGR1, STAT1, XAF1, OASL, OAS1, OAS2, IRF7, IRF6, USP18, GBP2, MX1
Interferon gamma signaling (R)	0.0074	72	17	0.0000	1.52E-11	TRIM22, HLA-DQA1, HLA-DRB5, HLA-DRB1, HLA-DPA1, CD44, HLA-DQB1, STAT1, HLA-DPB1, HLA-DRA, OASL, OAS1, OAS2, IRF7, IRF6, GBP2, GBP1
Inflammatory bowel disease (IBD) (K)	0.0068	66	13	0.0000	6.70E-08	GATA3, HLA-DQA1, HLA-DRB5, HLA-DRB1, HLA-DPA1, HLA-DQB1, HLA-DMA, HLA-DMB, STAT4, STAT1, HLA-DPB1, IL4R, HLA-DRA
Allograft rejection (K)	0.0039	38	10	0.0000	2.37E-07	PRF1, HLA-DQA1, HLA-DRB5, HLA-DRB1, HLA-DPA1, HLA-DQB1, HLA-DMA, HLA-DMB, HLA-DPB1, HLA-DRA
Graft-versus-host disease (K)	0.0043	42	10	0.0000	5.03E-07	PRF1, HLA-DQA1, HLA-DRB5, HLA-DRB1, HLA-DPA1, HLA-DQB1, HLA-DMA, HLA-DMB, HLA-DPB1, HLA-DRA
Asthma (K)	0.0032	31	9	0.0000	5.03E-07	HLA-DQA1, HLA-DRB5, HLA-DRB1, HLA-DPA1, HLA-DQB1, HLA-DMA, HLA-DMB, HLA-DPB1, HLA-DRA
Cell adhesion molecules (CAMs) (K)	0.0148	144	16	0.0000	8.00E-07	ALCAM, SDC4, SDC2, HLA-DQA1, HLA-DRB5, HLA-DRB1, HLA-DPA1, HLA-DQB1, HLA-DMA, HLA-DMB, HLA-DPB1, CDH1, NRCAM, SELL, HLA-DRA, CD6
Antigen processing and presentation (K)	0.0080	78	11	0.0000	1.02E-05	HLA-DQA1, HLA-DRB5, HLA-DRB1, HLA-DPA1, HLA-DQB1, HLA-DMA, HLA-DMB, HLA-DPB1, HSPA1A, HSPA2, HLA-DRA
Intestinal immune network for IgA production (K)	0,0049	48	9	0.0000	1.15E-05	HLA-DQA1, HLA-DRB5, HLA-DRB1, HLA-DPA1, HLA-DQB1, HLA-DMA, HLA-DMB, HLA-DPB1, HLA-DRA
Systemic lupus erythematosus (K)	0.0138	135	13	0.0000	5.28E-05	C3, HLA-DQA1, HLA-DRB5, HLA-DRB1, HLA-DPA1, HLA-DQB1, HLA-DMA, HLA-DMB, HLA-DPB1, HIST1H2AE, HIST1H2BG, HIST1H2BD, HLA-DRA
TCR signaling (R)	0.0067	65	8	0.0000	8.54E-04	PAG1, HLA-DQA1, HLA-DRB5, HLA-DRB1, HLA-DPA1, HLA-DQB1, HLA-DPB1, HLA-DRA
MHC class II antigen presentation (R)	0.0091	89	9	0.0001	0.001	HLA-DQA1, HLA-DRB5, HLA-DRB1, HLA-DPA1, HLA-DQB1, HLA-DMA, HLA-DMB, HLA-DPB1, HLA-DRA
Rheumatoid arthritis (K)	0.0092	90	9	0.0001	0.001	HLA-DQA1, HLA-DRB5, HLA-DRB1, HLA-DPA1, HLA-DQB1, HLA-DMA, HLA-DMB, HLA-DPB1, HLA-DRA
Phagosome (K)	0.0158	154	11	0.0002	0.003	C3, HLA-DQA1, HLA-DRB5, HLA-DRB1, HLA-DPA1, HLA-DQB1, HLA-DMA, HLA-DMB, HLA-DPB1, CLEC7A, HLA-DRA
Costimulation by the CD28 family (R)	0.0064	62	7	0.0002	0.003	HLA-DQA1, HLA-DRB5, HLA-DRB1, HLA-DPA1, HLA-DQB1, HLA-DPB1, HLA-DRA
IL12 signaling mediated by STAT4 (N)	0.0031	30	5	0.0003	0.005	PRF1, HLA-DRB1, STAT4, HLA-DRA, ETV5
Validated transcriptional targets of TAp63 isoforms (N)	0.0050	49	6	0.0003	0.006	EGR2, CDKN1A, MFGE8, NQO1, IGFBP3, PMAIP1
T-cell activation (P)	0.0083	81	7	0.0009	0.01	HLA-DQA1, HLA-DPA1, HLA-DMA, HLA-DMB, ITPR1, HLA-DRA, PIK3CD
Direct p53 effectors (N)	0.0135	132	9	0.0009	0.01	ATF3, TGFA, SFN, CDKN1A, DUSP1, HSPA1A, CD82, IGFBP3, PMAIP1
ECM–receptor interaction (K)	0.0089	87	7	0.0013	0.01	SDC4, FN1, COL1A1, COL1A2, CD44, ITGA7, LAMB3
IL4-mediated signaling events (N)	0.0066	64	6	0.0013	0.02	EGR2, PARP14, COL1A1, COL1A2, IL13RA2, IL4R
Proteoglycans in cancer (K)	0.0209	204	11	0.0016	0.02	CBLB, ANK3, SDC4, SDC2, FN1, CDKN1A, CD44, FLNB, ITPR1, HPSE, PIK3CD
p53 signaling pathway (K)	0.0070	68	6	0.0018	0.02	SFN, CDKN1A, CD82, SESN3, IGFBP3, PMAIP1
Calcineurin-regulated NFAT-dependent transcription in lymphocytes (N)	0.0048	47	5	0.0020	0.02	CBLB, GATA3, EGR1, EGR2, GBP3
Apoptotic execution phase (R)	0.0048	47	5	0.0020	0.02	GSN, TJP2, CDH1, H1F0, DSP
Proteoglycan syndecan-mediated signaling events (N)	0.0004	4	2	0.0026	0.03	SDC4, SDC2
ErbB1 downstream signaling (N)	0.0103	100	7	0.0028	0.03	NCKAP1, EPS8, SFN, EGR1, DUSP1, CHN2, STAT1

Gene annotation and networks were generated with the Reactome Functional Interaction Cytoscape plugin (http://www.cytoscape.org/)

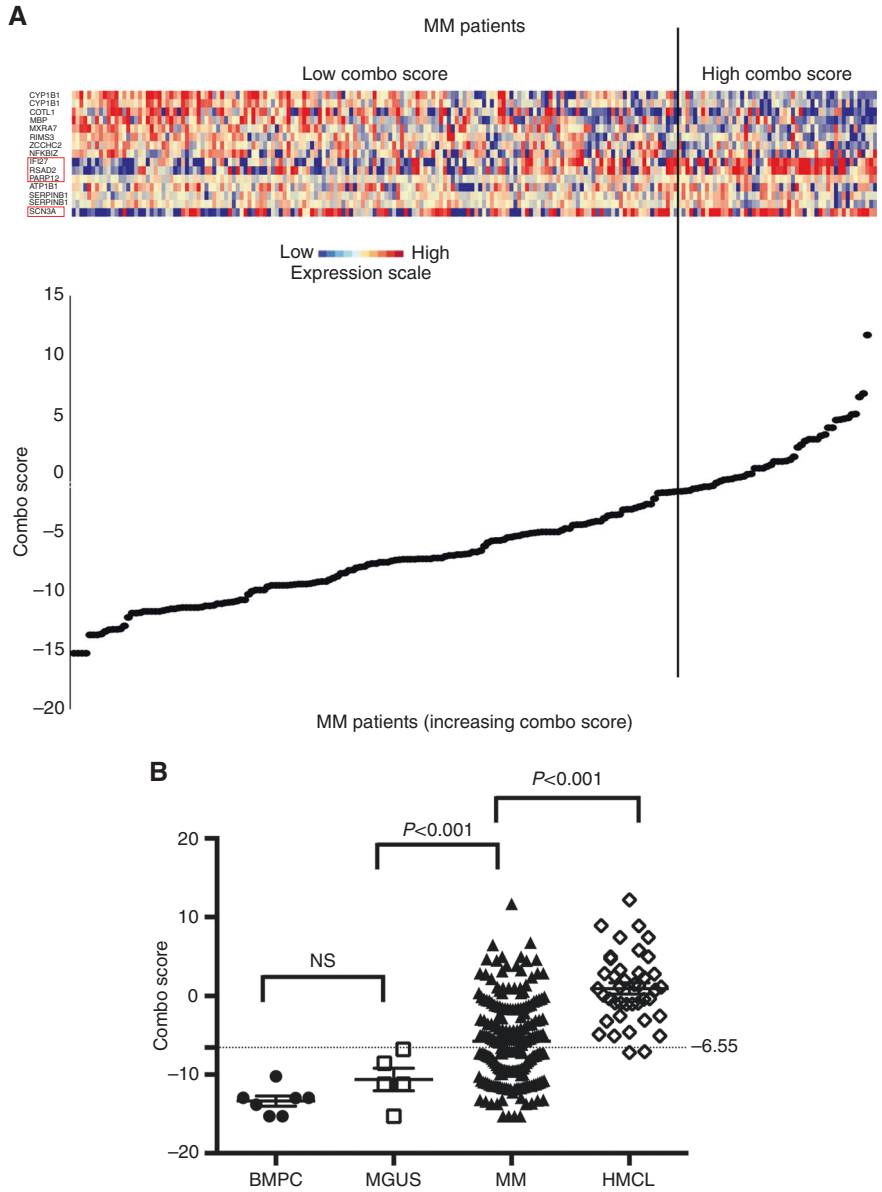

Fig. 1 Clustergram of the signals of the 15 genes used to build the Combo score in myeloma cells of 206 previously untreated patients. **a** The signals of the 15 probe sets in MMCs of 206 patients, ordered by increasing Combo score, are displayed from low (deep blue) to high (deep red) expression. Among the 15 probe sets, the genes associated with a poor outcome are identified by a red frame. **b** Combo score in normal bone marrow plasma cells ($n = 7$), in premalignant plasma cells of patients with monoclonal gammopathy of undetermined significance (MGUS, $n = 5$), in multiple myeloma cells of patients with intramedullary MM ($n = 206$), and in human myeloma cell lines ($n = 40$)

combination is associated with high toxicity, including thrombocytopenia (67%), lymphopenia (53%), diarrhoea (26%), and asthenia or fatigue (24%). Several other ongoing trials are evaluating panobinostat in combination with other partners (both standard-of-care agents and targeted therapies) for newly diagnosed or relapsing/refractory MM patients[19].

Recently, Matthews et al. investigated the potential of combining panobinostat with a BH3-only mimetic (ABT-737), recombinant human tumor necrosis factor-related apoptosis-inducing ligand (rhTRAIL), or 5-azacitidine, in vivo, using the Vk*MYC transgenic MM mouse model[22]. HDACi/rhTRAIL or HDACi/ABT-737 combinations are associated with important drug-induced toxicity in vivo. In contrast, HDACi and DNMTi demonstrated a significant reduction of tumor load and prolonged survival of mice without observing major toxicity[22, 23]. In patients with solid cancers or advanced hematological malignancies, HDACi and DNMTi combination was well tolerated[24] and suggested promising activity in MDS, AML[16, 24, 25], and refractory advanced non-small cell lung cancer[26]. Together, these observations suggest that targeting the aberrant tumor-specific epigenetic program simultaneously with DNMTi and HDACi treatment could have therapeutic interest in MM. However, identification of biomarkers predictive for sensitivity of MMCs to epigenetic therapies remains an important objective to improve clinical trials. We recently reported gene expression (gene expression profiling (GEP))-based risk scores to predict the sensitivity of MMCs to DNMTi[27, 28] and HDACi[28]. Since HDACi and DNMTi combination have potential therapeutic value in MM, we aimed to build a GEP-based score that could be useful to design future epigenetic-targeted combination trials. In addition, we investigated the changes in GEP upon HDACi/DNMTi treatment in

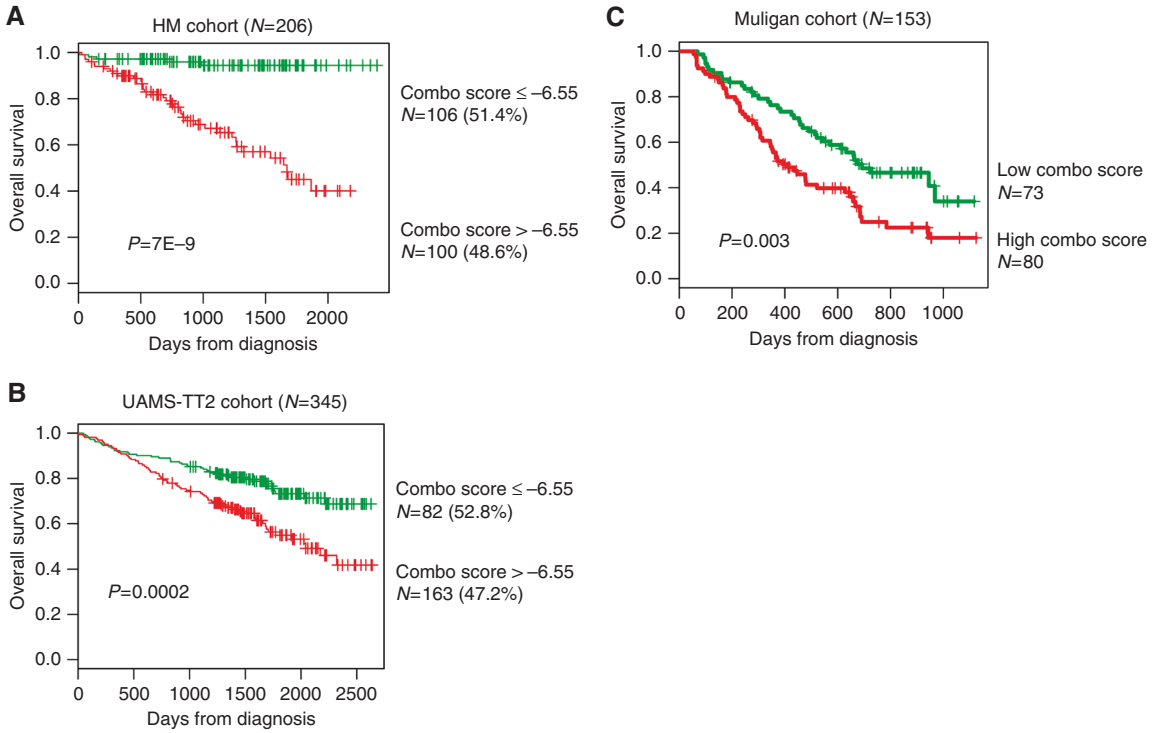

Fig. 2 Prognostic value of Combo score in multiple myeloma. **a** Patients of the HM cohort were ranked according to increased Combo score and a maximum difference in OS was obtained with Combo score = −6.55 splitting patients into high-risk (48.6%) and low-risk (51.4%) groups. **b** The prognostic value of Combo score was validated using an independent cohort of 345 patients from UAMS treated with TT2 therapy (UAMS-TT2 cohort). The parameters to compute the Combo score of patients of UAMS-TT2 cohort and the proportions delineating the two prognostic groups were those defined in the HM cohort. **c** The prognostic value of Combo score was validated in a cohort of 188 patients at relapse treated with bortezomib monotherapy (Mulligan cohort)[40]

order to identify mechanisms underlying the enhanced anti-MM activity using human MM cell lines and the 5T33MM model.

MATERIALS AND METHODS

Human myeloma cell lines (HMCLs) and primary MM cells of patients

HMCLs ($N = 40$) were obtained as previously described[29–34] or purchased from DSMZ and American Type Culture Collection. Microarray data are deposited in the ArrayExpress public database (accession numbers E-TABM-937 and E-TABM-1088). Patients presenting with previously untreated MM ($N = 206$) or monoclonal gammopathy of undetermined significance (MGUS; $N = 5$) at the university hospitals of Heidelberg and Montpellier, as well as 7 healthy donors have been included in the study approved by the ethics committee of Montpellier and Heidelberg after written informed consent in accordance with the Declaration of Helsinki. Clinical parameters and treatment regimens of the MM patients included in the Heidelberg–Montpellier (HM) cohort were previously described[35]. GEP of purified MMCs was assayed using Affymetrix U133 2.0 plus microarrays (Affymetrix, Santa Clara, CA, USA) as described[36] and data normalized using the MAS5 Affymetrix algorithm. The .CEL and MAS5 files are deposited in the ArrayExpress public database (http://www.ebi.ac.uk/arrayexpress/), under accession number E-MTAB-362. We also used publicly available MAS5 normalized GEP data (GEO, http://www.ncbi.nlm.nih.gov/geo/, accession number GSE2658) from purified MMCs of a cohort of 345 patients treated with total therapy 2 protocol (UAMS-TT2 cohort) at the University of Arkansas for Medical Sciences (UAMS, Little Rock, USA)[37]. t(4;14) translocation was evaluated using *MMSET* spike expression[38] and del17p13 surrogated by *TP53* probe set signal[39] for UAMS-TT2 patients. We also used Affymetrix data of 152 relapsed MM patients subsequently treated with bortezomib (GSE9782) from the study of Mulligan et al.[40] Gene expression data of normal memory B cells (MB), preplasmablasts, plasmablasts, and early plasma cells[41, 42] are deposited in the ArrayExpress databases under accession numbers E-MEXP-2360 and E-MEXP-3034.

Identification of genes deregulated by the HDACi/DNMTi combination

HMCLs (XG-5, XG-6, XG-7, XG-12, XG-19, XG-20, OPM2, RPMI8226, and LP1) were treated with 0.5 µmol/L decitabine (Sigma, St Louis, MO) for 7 days in RPMI 1640, 10% fetal bovine serum supplemented with interleukin (IL)-6 for IL-6-dependent HMCLs. During the last 24 h, 0.33 µmol/L trichostatin A (TSA; Sigma) was added as described by Heller et al.[43]Whole-genome GEP was assayed with Affymetrix U133 2.0 plus microarrays (Affymetrix).

C57BL/KaLwRij mice were purchased from Harlan CPB (Horst, The Netherlands). Mice were housed according to the conditions approved by the Ethical Committee for Animal Experiments of the Vrije Universiteit Brussel (license no. LA1230281). At day 0, naive C57BL/KaLwRij mice were injected with 5×10^5 5T33MM cells. After establishment of disease (day 16), mice were treated with the combination of decitabine (0.2 mg/kg) (intraperitoneal injection, daily) and quisinostat (1.5 mg/kg) (subcutaneous injection, once every other day) or vehicle. Compounds were kindly provided by Johnson & Johnson (Beerse, Belgium) and used as a filter-sterilized 10% hydroxypropyl-cyclodextran suspension. After 5 days, mice were sacrified and the bone marrow was isolated from hind legs. For mRNA analysis, tumor cells were purified by depletion of CD11b+ contaminating cells. Cytospins were made before and after depletion to count the percentage of plasma cells as described previously[23]. Samples with >95% plasma cells ($N = 4$

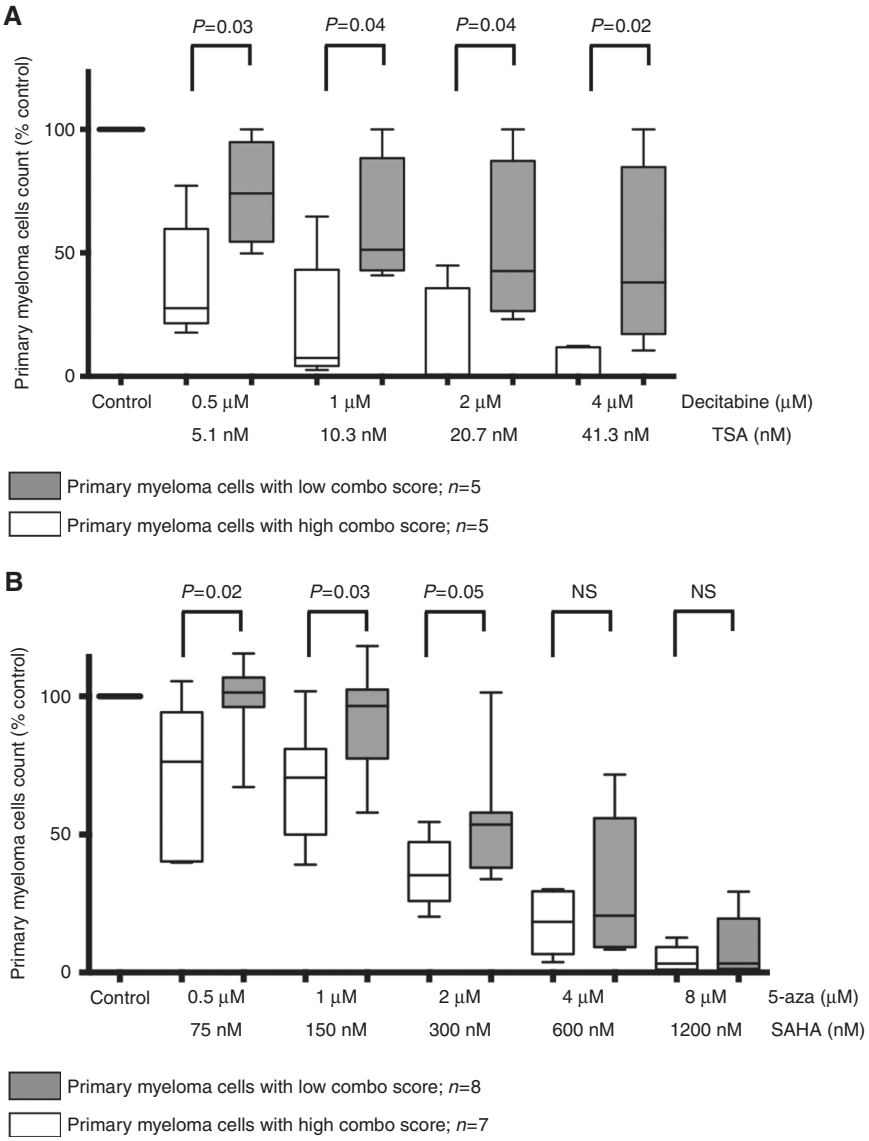

Fig. 3 Combo score predicts for sensitivity of primary myeloma cells of patients to HDACi/DNMTi combined treatment. **a** Mononuclear cells from tumor samples of 10 patients with MM were cultured for 4 days in the presence of IL-6 (2 ng/ml) with or without graded decitabine and TSA concentrations. At day 4 of culture, the count of viable $CD138^+$ MMCs was determined using flow cytometry. The gray columns represent the mean ± SD of primary myeloma cell counts (expressed as the percentage of the count without adding drugs) of the five patients with a low Combo score and the white columns that of the five patients with a high Combo score. **b** 5-Azacitidine and SAHA combination was also investigated using samples of 15 myeloma patients. The gray columns represent the mean ± SD of primary myeloma cell counts (expressed as the percentage of the count without adding drugs) of the 8 patients with a low Combo score and the white columns that of the 7 patients with a high Combo score

in each group) were used for RNA isolation using the RNeasy Kit (Qiagen, Venlo, The Netherlands). RNA was further processed and hybridized to the Mouse Genome 430 2.0 Array (Affymetrix, Santa Clara, CA, USA) as previously described[23, 27]. Microarray data are available at ArrayExpress database (Accession number: E-MTAB-3178).

Sensitivity of primary myeloma cells to HDACi/DNMTi combination
Primary myeloma cells of 10 patients were cultured with or without graded concentrations of decitabine and TSA. Primary myeloma cells of 15 patients were cultured with or without graded concentrations of 5-azacitidine (Sigma) and vorinostat (SAHA) (Sigma). MMC cytotoxicity was evaluated using anti-CD138-PE monoclonal antibody (mAb; Immunotech, Marseille, France) as described[27, 44]. Results were analyzed using GraphPad Prism (http://www.graphpad.com/scientific-software/prism/).

Statistical analysis
Gene expression data were analyzed using the SAM (Significance Analysis of Microarrays) software[45] as published[38]. The statistical significance of differences in OS between groups of patients was calculated by log-rank test. Multivariate analysis was performed using the Cox proportional hazards model. Survival curves were plotted using the Kaplan–Meier method. All these analyses have been done with R.2.10.1 (http://www.r-project.org/), bioconductor version 2.5 and Genomicscape (http://www.genomicscape.com)[46]. A histone acetylation/DNA methylation risk score (termed Combo score) was built using our previously published methodology with the decitabine/HDACi combination deregulated prognostic genes[27, 28]. Briefly, the Combo score was constructed as the sum of the Cox model beta coefficients of each of the decitabine/HDACi combination deregulated genes with a prognostic value, weighted by ±1 according to the patient MMC signal above or below the probeset maxstat value[27, 28, 38]. Significantly

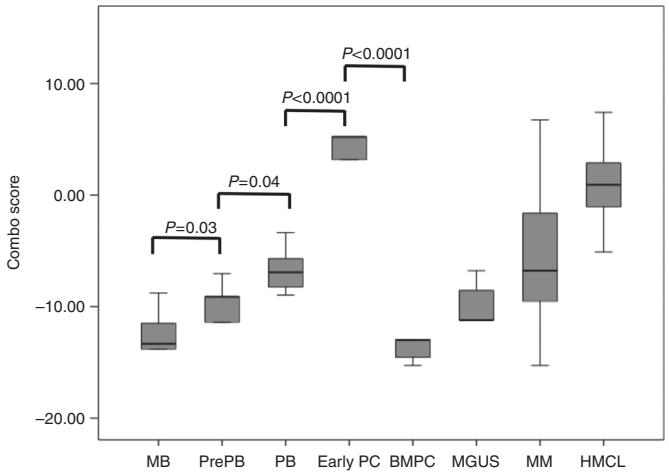

Fig. 4 Combo score in normal plasma cell differentiation. Combo score in normal memory B cells (MB, $n = 5$), normal preplasmablasts (PrePB, $n = 5$), normal plasmablasts (PB, $n = 5$), normal early plasma cells (Early PC, $n = 5$), normal bone marrow plasma cells ($n = 5$), in premalignant plasma cells of patients with monoclonal gammopathy of undetermined significance (MGUS, $n = 5$), multiple myeloma cells of patients with intramedullary MM ($n = 206$), and human myeloma cell lines ($n = 40$)

enriched pathways were identified using Reactome functional interaction map. Murine orthologs of HMCL genes were identified using OrthoRetriever tool (https://lighthouse.ucsf.edu/orthoretriever/). Gene set enrichment analysis was carried out by computing overlaps with canonical pathways and gene ontology gene sets obtained from the Broad Institute[47]. Clustering was performed and visualized with Cluster and TreeView[48].

Real-time reverse transcriptase PCR (RT-PCR)

RNA was converted to cDNA using the Qiagen's QuantiTect Rev. Transcription Kit (Qiagen, Hilden, Germany). The assays-on-demand primers and probes and the TaqMan Universal Master Mix were used according to the manufacturer's instructions (Applied Biosystems, Courtaboeuf, France). The measurement of gene expression was performed using the Roche LC480 Sequence Detection System. For each primer, serial dilutions of standard cDNA were amplified to create a standard curve, and values of unknown samples were estimated relative to this standard curve in order to assess PCR efficiency. Ct values were obtained for glyceraldehyde 3-phosphate dehydrogenase (GAPDH) and the respective genes of interest during the log phase of the cycle. Gene expression was normalized to that of GAPDH (ΔCt = Ct gene of interest−Ct GAPDH) and compared with the values obtained for a known positive control using the following formula: $100/2^{\Delta\Delta Ct}$ where ΔΔCt = ΔCt unknown −ΔCt positive control.

Immunophenotypic analyses

For immunophenotypic analysis, the Cytofix/Cytoperm Kit (BD Biosciences) was used for intracellular staining of IRF-4 (clone IRF4.3E4 from BioLegend (San Diego, CA, USA)) or MYC (clone #12189, Cell Signaling). Flow cytometric analysis was performed with a FORTESSA cytometer using FACSDiva 6.1 (Becton Dickinson, San Jose, CA, USA). The Kaluza software (Beckman Coulter) was used for data analysis. The fluorescence intensity of the cell populations was quantified using the staining index formula: [mean fluorescence intensity (MFI) obtained for a given mAb minus MFI obtained with a control mAb]/[2 times the standard deviation of the MFI obtained with the same control mAb][49].

RESULTS

Identification of genes with deregulated expression by decitabine and HDACi combination and associated with a prognostic value in MM

Using gene expression microarrays, we analyzed gene expression changes in HMCLs after (Supplementary Table S1) combination treatment with sub-lethal doses of decitabine and TSA[43]. HDACi/DNMTi treatment resulted in a significant upregulation of 375 genes (SAM supervised paired analysis, false discovery rate (FDR) < 5%; Supplementary Table S2) without significant downregulated genes. Reactome analysis revealed a significant enrichment of genes involved in immunological and inflammatory diseases, p53 and TAp63 anti-oncogenic signaling pathways, and cell-to-cell communication signals (Table 1). We also used the syngeneic, immunocompetent 5T33MM to study the in vivo transcriptional response of MM cells to HDACi/DNMTi combination as previously described[23]. Similar to the HMCL, the sub-lethal doses showing minimal effects on BM plasmacytosis ensuring the yield of good-quality RNA were used (data not shown). In vivo HDACi/DNMTi treatment resulted in a significant deregulation of 415 genes (SAM supervised paired analysis, FDR < 5%; Supplementary Table S3). To identify genes commonly deregulated by the combination in vitro and in vivo, we compared results obtained with the HMCLs and the 5T33MM model. A list of 52 common HDACi/DNMTi deregulated genes was identified (Supplementary Table S4). Using Maxstat R function and Benjamini–Hochberg multiple testing correction[38], we then investigated the association between the expression levels of these 52 genes and patient prognosis in order to find genes regulated by HDAC and DNMT that could have an important function in MM pathophysiology. Among the 52 genes, 4 genes had a bad prognostic value and 11 a good one in our cohort of 206 newly diagnosed patients (HM cohort) (Supplementary Table S5). The prognostic information of HDACi/DNMTi combination deregulated genes was gathered in a Combo score as described in the Materials and methods section (Fig. 1a). Combo score values in normal, premalignant, or malignant plasma cells are displayed in Fig. 1b. The Combo score value was not significantly different in plasma cells from MGUS patients compared to normal BM plasma cells (BMPCs). However, MMCs of patients have a significantly higher Combo score than plasma cells from MGUS patients ($P < 0.001$) and HMCLs had the highest score ($P < 0.001$) (Fig. 1b). Investigating the Combo score in the eight groups of the molecular classification of MM, the Combo score was significantly higher in the proliferation and hyperdiploid subgroups ($P < 0.001$, $P = 0.001$, and $P < 0.001$, respectively) and significantly lower in the low bone disease, CD2, and MY subgroups ($P = 0.02$, $P = 0.003$, and $P = 0.002$, respectively)[50] (Supplementary Figure S1).

Evaluation of the prognostic significance of the Combo score

Using a maxstat analysis for OS[51], the Combo score was significantly associated with high-risk myeloma in the two independent cohorts of newly diagnosed patients, namely, HM and UAMS-TT2 (Fig. 2a, b). Maxstat statistic test split the HM patient cohort into two groups: a high-risk group of 48.6 % patients (Combo score > −6.55) with a 54.9 months median OS and a low-risk group of 51.4% patients (Combo score ≤ −6.55) with not reached median survival ($P = 7E{-}9$; Fig. 2a). In the UAMS-TT2 cohort, a Combo score >−6.55 is also associated with a high risk ($P = 0.002$; Fig. 2b) in 47.2% of the patients. Next, we investigated whether the Combo score could also have a prognostic value in relapsed patients. Using the Mulligan cohort, including patients treated with bortezomib monotherapy after relapse, the Combo score kept prognostic value ($P = 0.003$; Fig. 2c).

The prognostic value of the Combo score was then compared to usual prognostic factors (β2M, ISS, t(4;14), and del17p) and the published GEP-based risk scores, i.e., UAMS-HRS[52], IFM score[53], RS score[54], proliferation scores, GPI[35], and scores surrogating

Table 2. Top gene set significantly enriched in untreated compared to MMC (n=9) treated by DNMTi/HDACi combination

Gene set name	Genes in gene set (K)	Description	Genes in overlap (k)	k/K	*P*-value	FDR *q*-value
HELLER_HDAC_TARGETS_SILENCED_BY_METHYLATION_UP	461	Genes upregulated in multiple myeloma (MM) cell lines treated with both decitabine [PubChem=451668] TSA [PubChem=5562]	49	0.1063	8.57E-31	4.06E-27
SENESE_HDAC3_TARGETS_DN	536	Genes downregulated in U2OS cells (osteosarcoma) upon knockdown of HDAC3 [GeneID=8841] by RNAi	41	0.0765	1.58E-20	1.07E-17
PILON_KLF1_TARGETS_DN	1972	Genes downregulated in erythroid progenitor cells from fetal livers of E13.5 embryos with KLF1 [GeneID=10661] knockout compared to those from the wild-type embryos	78	0.0396	7.34E-20	4.35E-17
HELLER_SILENCED_BY_METHYLATION_DN	105	Genes downregulated in at least one of the three multiple myeloma (MM) cell lines treated with the DNA hypomethylating agent decitabine (5-aza-2'-deoxycytidine) [PubChem=451668]	20	0.1905	2.33E-18	1.03E-15
HELLER_HDAC_TARGETS_SILENCED_BY_METHYLATION_DN	281	Genes downregulated in multiple myeloma (MM) cell lines treated with both decitabine [PubChem=451668] TSA [PubChem=5562]	29	0.1032	2.39E-18	1.03E-15
MEISSNER_BRAIN_HCP_WITH_H3K4ME3_AND_H3K27ME3	1069	Genes with high-CpG-density promoters (HCP) bearing histone H3 dimethylation at K4 (H3K4me2) and trimethylation at K27 (H3K27me3) in the brain	52	0.0486	4.33E-17	1.47E-14
HELLER_HDAC_TARGETS_UP	317	Genes upregulated in at least one of the three multiple myeloma (MM) cell lines by TSA [PubChem=5562]	29	0.0915	6.26E-17	1.98E-14
NUYTTEN_EZH2_TARGETS_UP	1037	Genes upregulated in PC3 cells (prostate cancer) after knockdown of EZH2 [GeneID=2146] by RNAi	49	0.0473	1.13E-15	2.97E-13
NUYTTEN_EZH2_TARGETS_DN	1024	Genes downregulated in PC3 cells (prostate cancer) after knockdown of EZH2 [GeneID=2146] by RNAi	46	0.0449	5.41E-14	1.03E-11
HELLER_SILENCED_BY_METHYLATION_UP	282	Genes upregulated in at least one of the three multiple myeloma (MM) cell lines treated with the DNA hypomethylating agent decitabine (5-aza-2'-deoxycytidine) [PubChem=451668]	24	0.0851	1.50E-13	2.49E-11
CHICAS_RB1_TARGETS_CONFLUENT	567	Genes upregulated in confluent IMR90 cells (fibroblast) after knockdown of RB1 [GeneID=5925] by RNAi	33	0.0582	2.26E-13	3.45E-11
HELLER_HDAC_TARGETS_DN	292	Genes downregulated in at least one of the three multiple myeloma (MM) cell lines by TSA [PubChem=5562]	24	0.0822	3.20E-13	4.74E-11
DANG_BOUND_BY_MYC	1103	Genes whose promoters are bound by MYC [GeneID=4609], according to MYC Target Gene Database	46	0.0417	7.35E-13	9.56E-11
ZHAN_MULTIPLE_MYELOMA_CD1_VS_CD2_UP	66	Genes upregulated in CD-1 compared to CD-2 cluster of multiple myeloma samples	13	0.197	1.32E-12	1.53E-10
WEI_MYCN_TARGETS_WITH_E_BOX	795	Genes whose promoters contain E-box motifs and whose expression changed in MYCN-3 cells (neuroblastoma) upon induction of MYCN [GeneID=4613]	37	0.0465	6.23E-12	6.71E-10
MARTINEZ_TP53_TARGETS_DN	593	Genes downregulated in mice with skin-specific knockout of TP53 [GeneID=7157]	31	0.0523	1.89E-11	1.79E-09
MARTINEZ_RB1_TARGETS_UP	673	Genes upregulated in mice with skin-specific knockout of RB1 [GeneID=5925] by Cre-lox	32	0.0475	1.00E-10	7.29E-09
PUJANA_ATM_PCC_NETWORK	1442	Genes constituting the ATM-PCC network of transcripts whose expression positively correlated (Pearson correlation coefficient, PCC≥0.4) with that of ATM [GeneID=472] across a compendium of normal tissues	49	0.034	1.75E-10	1.23E-08

Table 2 continued

Gene set name	Genes in gene set (K)	Description	Genes in overlap (k)	k/K	*P*-value	FDR *q*-value
SHAFFER_IRF4_TARGETS_IN_MYELOMA_VS_MATURE_B_LYMPHOCYTE	101	IRF4 [GeneID=3662] target genes up-regulated in primary myeloma vs. mature B lymphocytes	13	0.1287	3.57E-10	2.32E-08
MARTINEZ_RB1_AND_TP53_TARGETS_DN	591	Genes downregulated in mice with skin-specific double knockout of both RB1 and TP53 [GeneID=5925;7157] by Cre-lox	29	0.0491	3.71E-10	2.37E-08
SENESE_HDAC1_TARGETS_UP	457	Genes upregulated in U2OS cells (osteosarcoma) upon knockdown of HDAC1 [GeneID=3065] by RNAi	25	0.0547	6.79E-10	3.92E-08
BILD_MYC_ONCOGENIC_SIGNATURE	206	Genes selected in supervised analyses to discriminate cells expressing c-Myc [GeneID=4609] from control cells expressing GFP	17	0.0825	8.63E-10	4.92E-08
CHICAS_RB1_TARGETS_GROWING	243	Genes upregulated in growing IMR90 cells (fibroblast) after knockdown of RB1 [GeneID=5925] by RNAi	18	0.0741	1.57E-09	8.46E-08
BENPORATH_CYCLING_GENES	648	Genes showing cell-cycle stage-specific expression [PMID=12058064]	29	0.0448	2.99E-09	1.48E-07
REACTOME_CELL_CYCLE	421	Genes involved in cell cycle	23	0.0546	3.36E-09	1.61E-07
CHICAS_RB1_TARGETS_SENESCENT	572	Genes upregulated in senescent IMR90 cells (fibroblast) after knockdown of RB1 [GeneID=5925] by RNAi	27	0.0472	3.44E-09	1.63E-07

response to treatment DM score[27] and HA score[28]. In univariate COX analysis, all of these factors had prognostic value (Supplementary Table S5). Compared two by two in multivariate COX analysis, Combo score, ISS, IFM score, t(4;14), GPI, DM score, HA score, and β2M remained independent in the HM cohort. In the UAMS-TT2 cohort, when compared two by two, Combo score tested with HRS, IFM score, t(4;14), del17p, RS, GPI, HA score, and DM score remained independent prognostic factors. When tested all together, Combo score, β2M, and RS remained independent in the HM cohort, whereas UAMS-HRS, t(4;14), and del17p were independent in the UAMS-TT2 cohort (Supplementary Table S6).

The Combo score is predictive for myeloma cell sensitivity to DNMTi and HDACi combination

The efficacy of the Combo score to predict sensitivity of myeloma cells to DNMTi/HDACi treatment was investigated using primary MMC of patients co-cultured with their bone marrow microenvironment in vitro[27, 28]. MMC of patients with a high Combo score ($n = 5$) were significantly more sensitive to decitabine and TSA combination than MMC of patients with a low Combo score ($n = 5$) (Fig. 3a). We confirmed these results using another DNMTi and HDACi association. Primary MMCs of patients with a high Combo score ($n = 7$) exhibited a significant higher sensitivity to the clinical grade inhibitors 5-azacitidine/SAHA combination than MMC of patients with a low Combo score ($n = 8$) (Fig. 3b). Altogether, these data indicated that patients with high risk identified using the Combo score could benefit from HDACi/DNMTi treatment.

MMC of patients with a low Combo score value are characterized by a mature BMPC gene signature, whereas patients with high Combo score have a proliferating and MYC-associated gene signatures

In order to evaluate whether different gene signatures could be identified comparing the high and low Combo score groups, we performed a gene set enrichment analysis (GSEA). MMC of patients with a low Combo score displayed a significant enrichment in genes associated with normal mature BMPCs (gene set: MOREAUX MULTIPLE MYELOMA BY TACI UP, $P < 0.0001$, Supplementary Figure S2 and Supplementary Table S7) and bone microenvironment dependence (gene sets: KEGG CYTOKINE CYTOKINE RECEPTOR INTERACTION, $P < 0.0001$, Supplementary Figure S2 and Supplementary Tables S8). In contrast, MMCs of patients with a high Combo score exhibited a significant enrichment in genes associated with proliferating plasmablastic progenitors (gene sets: WHITFIELD CELL CYCLE S, REACTOME CELL CYCLE $P < 0.0001$ and $P = 0.01$, Supplementary Figure S3 and Supplementary Tables S9 and S10), MYC deregulation (gene sets: ODONNEL TARGETS OF MYC, DANG MYC TARGETS UP, $P < 0.0001$ and 0.002, Supplementary Figure S3 and Supplementary Table S11 and S12), and transcription (gene set: REACTOME TRANSCRIPTION, $P < 0.0001$, Supplementary Figure S3 and supplementary Table S13). Investigating the Combo score in normal plasma cell differentiation, the Combo score value was significantly higher in preplasmablasts (PrePB, $P = 0.03$) compared to MB cells and in plasmablasts (PB, $P = 0.04$) compared to preplasmablasts (Fig. 4). Early plasma cells were found to have the highest score ($P < 0.001$) and the Combo score decreased drastically to the lowest value in mature BMPC ($P < 0.001$) (Fig. 4).

HDACi/DNMTi combination results in significant downregulation of IRF4 and MYC expression

Since MM patients with a high Combo score are characterized by deregulation of MYC target genes, we next investigated the link between DNMTi/HDACi combined treatment and MYC deregulation using nine different HMCLs. Interestingly, GSEA analysis underlined that DNMTi/HDACi treatment results in a significant downregulation of genes silenced by H3K27 and DNA methylation, HDAC, EZH2, IRF4, and MYC target genes, suggesting that the

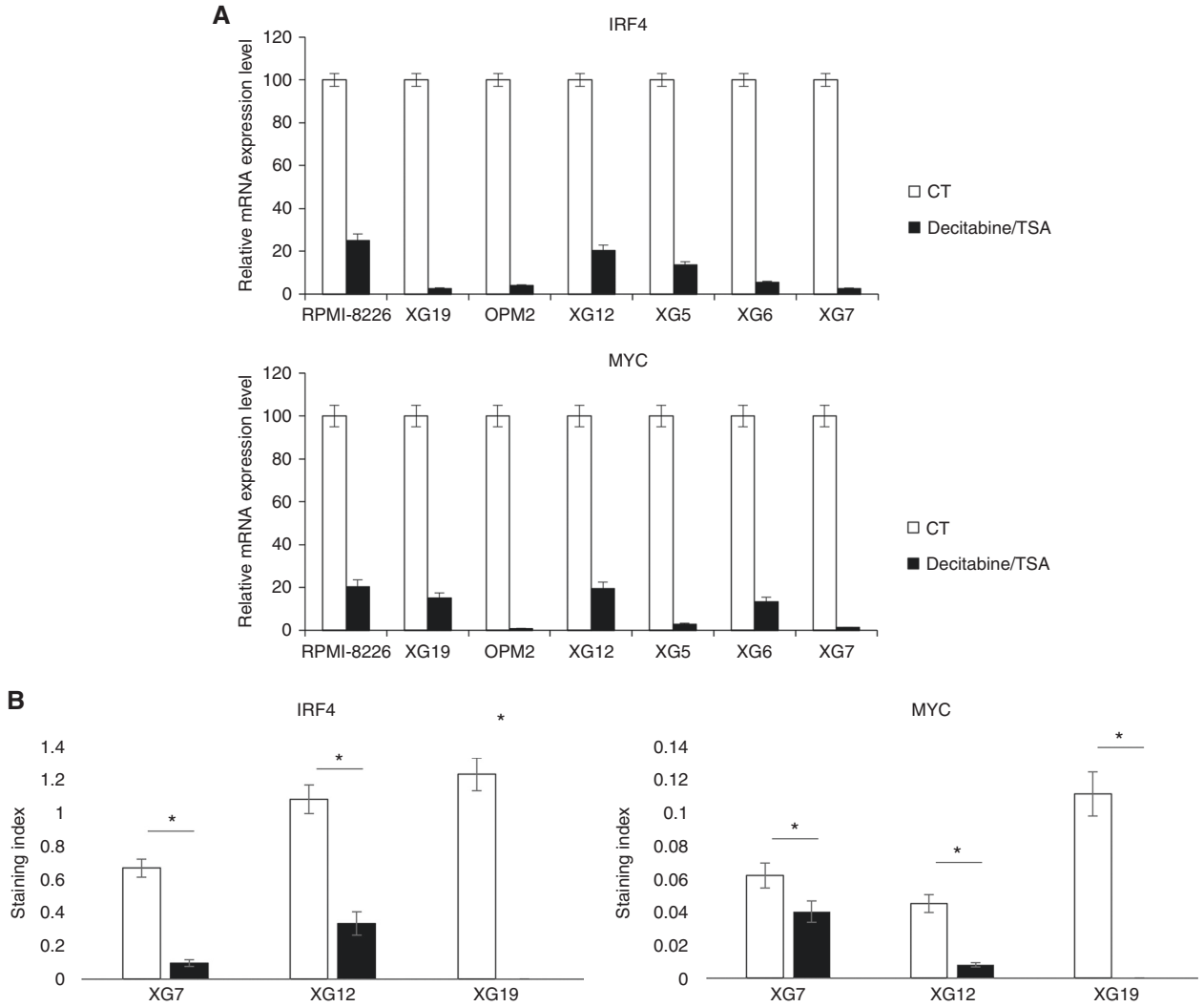

Fig. 5 HDACi/DNMTi induces a significant downregulation of IRF4 and MYC expression. **a** Seven HMCLs were treated for 7 days with decitabine (DNMTi) and TSA during the last 24 h. Data are the *MYC* and *IRF4* gene expression in treated HMCLs compared to the control (arbitrary signal = 100) assayed using real-time PCR. **b** Protein expression of MYC and IRF4 was assayed using flow cytometry in three HMCLs, namely XG7, XG12, and XG19

effects of the combination could be mediated by IRF4 and MYC downregulation (Table 2). *IRF4* and *MYC* downregulation after HDACi/DNMTi treatment was validated at the mRNA level by using QPCR (Fig. 5a) and at the protein level (Fig. 5b). Of note, this strong common downregulation of MYC and IRF4 expression was higher compared to DNMTi or HDACi treatment alone (Supplementary Figure S4A-B).

HDACi/DNMTi combination results in epigenetic reprogramming of MMCs

As we identified HDACi/DNMTi combined treatment is associated with MYC/IRF4 axis dysregulation thought to play a role in MM pathophysiology, we sought to determine whether HDACi/DNMTi treatment is associated with an epigenetic reprogramming of MMCs. Cluster analysis of the top 100 genes deregulated by HDACi/DNMTi (GSEA analysis) revealed that treated HMCLs cluster with normal BMPC, suggesting that HDACi/DNMTi combined treatment induced a normal BMPC gene program (Fig. 6). Altogether, these data indicate an epigenetic reprogramming of MMCs by HDACi/DNMTi combination, associated with MYC/IRF4 axis targeting and normal BMPC gene expression pattern induction.

DISCUSSION

Clinical trials suggested promising activity of HDACi/DNMTi combination in MDS, AML[16, 24, 25], and refractory advanced non-small cell lung cancer[26]. In MM, the oral HDACi panobinostat was recently approved by the US Food and Drug Administration for use in combination with bortezomib and dexamethasone in patients with relapsed MM[19]. In addition, ongoing trials are investigating the therapeutic interest of panobinostat with other agents including next-generation proteasome inhibitors (carfilzomib and ixazomib), IMiD and dexamethasone, bortezomib and IMiD, or monoclonal antibodies in relapsed/refractory MM patients[19]. Moreover, DNMTi and HDACi combination resulted in a significant anti-myeloma activity in the Vk*MYC transgenic MM and 5T33MM mouse models[22, 23]. Importantly, cooperation between histone modifications and DNA methylation is known to be important for the establishment of global epigenetic patterns as well as loci-specific gene regulation[55]. This crosstalk can be mediated by biochemical interactions between SET domain histone methyltransferases and DNMTs[55]. Only upregulated genes were identified in the HMCLs treated with DNMTi/HDACi compared with untreated HMCLs with a significant enrichment in genes involved in immunological and inflammatory diseases, p53 and TAp63 signaling pathways, and intercellular

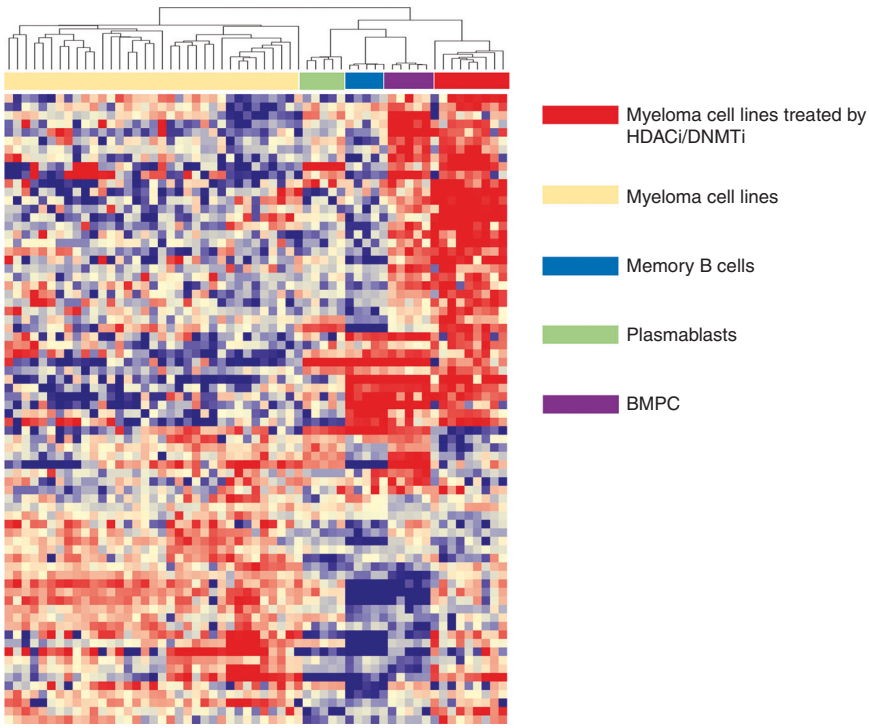

Fig. 6 HDACi/DNMTi induces a normal BMPC gene expression program in MM cells. The signals of the top 100 genes deregulated by HDACi/DNMTi in myeloma cell lines ($n = 49$), myeloma cell lines treated by DNMTi/HDACi ($n = 9$), normal memory B cells (MB, $n = 5$), normal plasmablasts (PB, $n = 5$), and normal bone marrow plasma cells ($n = 5$) are displayed from low (deep blue) to high (deep red) expression

communication signals. Significant induction of TP53 and TP53 homolog TAp63 target genes known to exert anti-oncogenic roles in cancers[56] and could participate in the MMC toxicity of HDACi/DNMTi combination.

In this study, we constructed a GEP-based Combo score that allows identification of high-risk patients associated with MMC's higher sensitivity to HDACi/DNMTi combination in vitro. Since HDACi/DNMTi combination are well tolerated[24] showing promising activity in cancers (including hematological malignancies[16, 24–26]) and have potential therapeutic value in MM[22, 23], the Combo score could enable the identification of MM patients who could benefit from this treatment.

The 15 genes used to build the Combo score, included 4 genes associated with a bad prognosis and 11 associated with a good prognosis (Fig. 1). Among these genes, some of them could highlight pathways involved in MM biology and sensitivity to DNMTi/HDACi combination. Patients with high Combo score, and poor survival, are characterized by a higher expression of the 4 bad prognostic genes and a lower expression of the 11 good ones in MMCs. Primary MMCs of patients with high Combo score can be efficiently targeted by the upregulation of gene products encoded by genes upregulated by HDACi/DNMTi, in particular the 11 good prognostic genes. A full understanding of the reason why the Combo score could predict for HDACi/DNMTi sensitivity will be provided by an extensive study of the function of the products encoded by HDACi/DNMTi-regulated genes in MMC survival and/or proliferation. Among them, *NFKBIZ* was identified. *NFKBIZ* codes the inhibitor of nuclear factor-κB (NFκB) (IκB) protein IκBζ. IκBζ is an atypical and mainly nuclear IκB protein working as a co-transcription factor of NFκB to modulate the expression of NFκB target genes[57]. NFκB is a major pathway involved in MMC survival and is activated by various gene mutations[58–60]. NFKBIZ overexpression was reported to induce cell death[61] and inhibit transcriptional activity of STAT3 with Mcl1 downregulation and apoptosis induction[62]. Mcl1 is known to be the major antiapoptotic protein involved in MMC survival[63, 64]. This significant overexpression of NFKBIZ after DNMTi/HDACi treatment was validated by quantitative RT-PCR in seven HMCLs (Supplementary Figure S5). As a significant enrichment in genes associated with proliferation was identified in MMC of patients with a high Combo score value, the higher sensitivity of high Combo score patients to DNMTi/HDACi combination could be explained by the fact that incorporation of DNMTi into DNA is restricted to cell cycling cells[3]. Furthermore, HDACi have been shown to induce G1 cell cycle arrest through dephosphorylation of retinoblastoma protein and increase expression of p53 and p21[9, 12, 14]. Using methylation-specific PCR, several studies have identified hypermethylation of tumor-suppressor genes including cyclin-dependent kinase inhibitors (CDKI, p15, and p16) and p14[65–67]. DNMTi/HDACi treatment induced p21 and p57 CDKI expression in MMC (Supplementary Table S2). Thus DNMTi/HDACi combination could be useful to induce the expression of major tumor-suppressor genes in MMC.

Furthermore, core histone proteins must be synthetized rapidly during the brief S-phase when a cell is dividing[68]. As a result, the histone mRNAs are highly cell cycle regulated, increasing 35-fold as cells enter S-phase and decreasing again at the end of S-phase[68]. Altogether, these data could clarify why MMC of high Combo score patients, distinguished by an active growth, can be efficiently targeted by HDACi/DNMTi treatment.

Most interestingly, HDACi/DNMTi treatment induced reprogramming of MMC through IRF4 and MYC axis targeting and induction of a normal BMPC gene expression program. IRF4 is a transcription factor critical for normal plasma cell development[69]. Abnormal activity of IRF4 linked to a translocation or the presence of superenhancers plays a key role in MM development[70, 71]. IRF4 is overexpressed in a subset a patients harboring t(6;14)(p25;q32) translocation[70]. MYC is an IRF4 target presenting prominent role in MM pathogenesis[69]. We report here that HDACi/DNMTi combination triggers a significant downregulation of MYC, IRF4, and several IRF4-MYC target genes. Interestingly, this strong common downregulation of MYC and IRF4 expression was not identified after DNMTi or HDACi treatment alone[27, 28]. It

was demonstrated that IMiDs could target IRF4 and MYC expression through binding to cereblon E3 ubiquitin ligase that promote proteasomal degradation of IKZF1 and IKZF3 transcriptional factors[72, 73].

These data suggest that DNMTi/HDACi could be of therapeutic interest in combination with IMiDs in high-risk MM with elevated Combo score value.

ACKNOWLEDGEMENTS

We thank the Microarray Core Facility of IRMB (http://irb.montp.inserm.fr/en/index.php?page=Plateau&IdEquipe=6). This work was supported by grants from French INCA (Institut National du Cancer) Institute (2012-109/087437 and PLBIO15-256), Languedoc Roussillon CRLR (R14026FF), LR-FEDER Hemodiag, Fondation de France (201400047510), ITMO Cancer (MM&TT), SIRIC Montpellier (INCa-DGOS-Inserm 6045), Kom Op tegen Kanker, Stichting tegen Kanker and Fonds voor Wetenschappelijk Onderzoek, Belgium, the German Federal Ministry of Education (BMBF) "CAMPSIMM" (01ES1103) and within the framework of the e:Med research and funding concept "CLIOMMICS" (01ZX1309), and the Deutsche Forschungsgemeinschaft (SFB/TRR79; subproject B1). L.H. is supported by a grant from Labex EpiGenMed.

AUTHOR CONTRIBUTIONS

A.B. and K.M. designed the research and wrote the paper. H.D., A.S., C.M.-T., L.V., S.B., G.C., and G.H. collected bone marrow samples and clinical data and participated in the writing of the paper. A.K., R.T., and J.-l.V. participated in the bioinformatics studies. N.R., G.R., and S.B. provided with technical assistance. K.V., L.H., and B.K. participated in the research and wrote the paper. E.D.B. and J.M. designed and supervised the research and wrote the paper. All authors read and approved the final manuscript.

ADDITIONAL INFORMATION

Supplementary information is available for this paper at https://doi.org/10.1038/s41416-018-0025-x.

Competing interests: The authors declare no competing interests.

REFERENCES

1. Heuck, C. J. et al. Myeloma is characterized by stage-specific alterations in DNA methylation that occur early during myelomagenesis. *J. Immunol.* **190**, 2966–2975 (2013).
2. Walker, B. A. et al. Aberrant global methylation patterns affect the molecular pathogenesis and prognosis of multiple myeloma. *Blood* **117**, 553–562 (2010).
3. Hollenbach, P. W. et al. A comparison of azacitidine and decitabine activities in acute myeloid leukemia cell lines. *PLoS ONE* **5**, e9001 (2010).
4. Maes, K. et al. Epigenetic modulating agents as a new therapeutic approach in multiple myeloma. *Cancers* **5**, 430–461 (2013).
5. Feng, R. et al. KD5170, a novel mercaptoketone-based histone deacetylase inhibitor, exerts antimyeloma effects by DNA damage and mitochondrial signaling. *Mol. Cancer Ther.* **7**, 1494–1505 (2008).
6. Hideshima, T. et al. Induction of differential apoptotic pathways in multiple myeloma cells by class-selective histone deacetylase inhibitors. *Leukemia* **28**, 457–460 (2013).
7. Kaiser, M. et al. The effects of the histone deacetylase inhibitor valproic acid on cell cycle, growth suppression and apoptosis in multiple myeloma. *Haematologica* **91**, 248–251 (2006).
8. Khan, S. B., Maududi, T., Barton, K., Ayers, J. & Alkan, S. Analysis of histone deacetylase inhibitor, depsipeptide (FR901228), effect on multiple myeloma. *Br. J. Haematol.* **125**, 156–161 (2004).
9. Lavelle, D., Chen, Y. H., Hankewych, M. & DeSimone, J. Histone deacetylase inhibitors increasep21(WAF1) and induce apoptosis of human myeloma cell lines independent of decreased IL-6 receptor expression. *Am. J. Hematol.* **68**, 170–178 (2001).
10. Minami, J. et al. Histone deacetylase 3 as a novel therapeutic target in multiple myeloma. *Leukemia* **28**, 680–689 (2013).
11. Mitsiades, C. S. et al. Transcriptional signature of histone deacetylase inhibition in multiple myeloma: biological and clinical implications. *Proc. Natl. Acad. Sci. USA* **101**, 540–545 (2004).
12. Mitsiades, N. et al. Molecular sequelae of histone deacetylase inhibition in human malignant B cells. *Blood* **101**, 4055–4062 (2003).
13. Catley, L. et al. NVP-LAQ824 is a potent novel histone deacetylase inhibitor with significant activity against multiple myeloma. *Blood* **102**, 2615–2622 (2003).
14. Neri, P., Bahlis, N. J. & Lonial, S. Panobinostat for the treatment of multiple myeloma. *Expert Opin. Investig. Drugs* **21**, 733–747 (2012).
15. Neri, P. et al. In vivo anti-myeloma activity and modulation of gene expression profile induced by valproic acid, a histone deacetylase inhibitor. *Br. J. Haematol.* **143**, 520–531 (2008).
16. Zhang, Q. L. et al. The proteasome inhibitor bortezomib interacts synergistically with the histone deacetylase inhibitor suberoylanilide hydroxamic acid to induce T-leukemia/lymphoma cells apoptosis. *Leukemia* **23**, 1507–1514 (2009).
17. Dimopoulos, M. et al. Vorinostat or placebo in combination with bortezomib in patients with multiple myeloma (VANTAGE 088): a multicentre, randomised, double-blind study. *Lancet Oncol.* **14**, 1129–1140 (2013).
18. Richardson, P. G. et al. PANORAMA 2: panobinostat in combination with bortezomib and dexamethasone in patients with relapsed and bortezomib-refractory myeloma. *Blood* **122**, 2331–2337 (2013).
19. Laubach, J. P., Moreau, P., San-Miguel, J. F. & Richardson, P. G. Panobinostat for the treatment of multiple myeloma. *Clin. Cancer Res.* **21**, 4767–4773 (2015).
20. Richardson, P. G. et al. Pomalidomide, bortezomib and low-dose dexamethasone in lenalidomide-refractory and proteasome inhibitor-exposed myeloma. *Leukemia* **31**, 2695–2701 (2017).
21. San-Miguel, J. F. et al. Panobinostat plus bortezomib and dexamethasone versus placebo plus bortezomib and dexamethasone in patients with relapsed or relapsed and refractory multiple myeloma: a multicentre, randomised, double-blind phase 3 trial. *Lancet Oncol.* **15**, 1195–1206 (2014).
22. Matthews, G. M. et al. Preclinical screening of histone deacetylase inhibitors combined with ABT-737, rhTRAIL/MD5-1 or 5-azacytidine using syngeneic Vk*MYC multiple myeloma. *Cell Death Dis.* **4**, e798 (2013).
23. Maes, K. et al. In vivo treatment with epigenetic modulating agents induces transcriptional alterations associated with prognosis and immunomodulation in multiple myeloma. *Oncotarget* **6**, 3319–3334 (2015).
24. Bots, M. & Johnstone, R. W. Rational combinations using HDAC inhibitors. *Clin. Cancer Res.* **15**, 3970–3977 (2009).
25. Fandy, T. E. et al. Early epigenetic changes and DNA damage do not predict clinical response in an overlapping schedule of 5-azacytidine and entinostat in patients with myeloid malignancies. *Blood* **114**, 2764–2773 (2009).
26. Juergens, R. A. et al. Combination epigenetic therapy has efficacy in patients with refractory advanced non-small cell lung cancer. *Cancer Discov.* **1**, 598–607 (2011).
27. Moreaux, J. et al. Development of gene expression-based score to predict sensitivity of multiple myeloma cells to DNA methylation inhibitors. *Mol. Cancer Ther.* **11**, 2685–2692 (2012).
28. Moreaux, J. et al. Gene expression-based prediction of myeloma cell sensitivity to histone deacetylase inhibitors. *Br. J. Cancer* **109**, 676–685 (2013).
29. Gu, Z. J. et al. Agonist anti-gp130 transducer monoclonal antibodies are human myeloma cell survival and growth factors. *Leukemia* **14**, 188–197 (2000).
30. Moreaux, J. et al. TACI expression is associated with a mature bone marrow plasma cell signature and C-MAF overexpression in human myeloma cell lines. *Haematologica* **92**, 803–811 (2007).
31. Moreaux, J. et al. A high-risk signature for patients with multiple myeloma established from the molecular classification of human myeloma cell lines. *Haematologica* **96**, 574–582 (2011).
32. Rebouissou, C. et al. A gp130 interleukin-6 transducer-dependent SCID model of human multiple myeloma. *Blood* **91**, 4727–4737 (1998).
33. Tarte, K. et al. Induced expression of B7-1 on myeloma cells following retroviral gene transfer results in tumor-specific recognition by cytotoxic T cells. *J. Immunol.* **163**, 514–524 (1999).
34. Zhang, X. G. et al. Reproducible obtaining of human myeloma cell lines as a model for tumor stem cell study in human multiple myeloma. *Blood* **83**, 3654–3663 (1994).
35. Hose, D. et al. Proliferation is a central independent prognostic factor and target for personalized and risk-adapted treatment in multiple myeloma. *Haematologica* **96**, 87–95 (2011).
36. De Vos, J. et al. Comparison of gene expression profiling between malignant and normal plasma cells with oligonucleotide arrays. *Oncogene* **21**, 6848–6857 (2002).
37. Barlogie, B. et al. Total therapy 2 without thalidomide in comparison with total therapy 1: role of intensified induction and posttransplantation consolidation therapies. *Blood* **107**, 2633–2638 (2006).
38. Kassambara, A. et al. Genes with a spike expression are clustered in chromosome (sub)bands and spike (sub)bands have a powerful prognostic value in patients with multiple myeloma. *Haematologica* **97**, 622–630 (2012).
39. Xiong, W. et al. An analysis of the clinical and biologic significance of TP53 loss and the identification of potential novel transcriptional targets of TP53 in multiple myeloma. *Blood* **112**, 4235–4246 (2008).
40. Mulligan, G. et al. Gene expression profiling and correlation with outcome in clinical trials of the proteasome inhibitor bortezomib. *Blood* **109**, 3177–3188 (2007).

41. Jourdan, M. et al. Characterization of a transitional preplasmablast population in the process of human B cell to plasma cell differentiation. *J. Immunol.* **187**, 3931–3941 (2011).
42. Jourdan, M. et al. An in vitro model of differentiation of memory B cells into plasmablasts and plasma cells including detailed phenotypic and molecular characterization. *Blood* **114**, 5173–5181 (2009).
43. Heller, G. et al. Genome-wide transcriptional response to 5-aza-2′-deoxycytidine and trichostatin a in multiple myeloma cells. *Cancer Res.* **68**, 44–54 (2008).
44. Mahtouk, K. et al. An inhibitor of the EGF receptor family blocks myeloma cell growth factor activity of HB-EGF and potentiates dexamethasone or anti-IL-6 antibody-induced apoptosis. *Blood* **103**, 1829–1837 (2004).
45. Cui, X. & Churchill, G. A. Statistical tests for differential expression in cDNA microarray experiments. *Genome Biol.* **4**, 210 (2003).
46. Kassambara, A. et al. GenomicScape: an easy-to-use web tool for gene expression data analysis. Application to investigate the molecular events in the differentiation of B cells into plasma cells. *PLoS Comput. Biol.* **11**, e1004077 (2015).
47. Subramanian, A. et al. Gene set enrichment analysis: a knowledge-based approach for interpreting genome-wide expression profiles. *Proc. Natl. Acad. Sci. USA* **102**, 15545–15550 (2005).
48. Eisen, M. B., Spellman, P. T., Brown, P. O. & Botstein, D. Cluster analysis and display of genome-wide expression patterns. *Proc. Natl. Acad. Sci. USA* **95**, 14863–14868 (1998).
49. Jourdan, M. et al. Differential effects of lenalidomide during plasma cell differentiation. *Oncotarget* **7**, 28096–28111 (2016).
50. Zhan, F. et al. The molecular classification of multiple myeloma. *Blood* **108**, 2020–2028 (2006).
51. Hothorn, T. & Lausen, B. On the exact distribution of maximally selected rank statistics. *Comput. Stat. Data Anal.* **43**, 121–137 (2003).
52. Shaughnessy, J. D. Jr. et al. A validated gene expression model of high-risk multiple myeloma is defined by deregulated expression of genes mapping to chromosome 1. *Blood* **109**, 2276–2284 (2007).
53. Decaux, O. et al. Prediction of survival in multiple myeloma based on gene expression profiles reveals cell cycle and chromosomal instability signatures in high-risk patients and hyperdiploid signatures in low-risk patients: a study of the Intergroupe Francophone du Myelome. *J. Clin. Oncol.* **26**, 4798–4805 (2008).
54. Reme, T., Hose, D., Theillet, C. & Klein, B. Modeling risk stratification in human cancer. *Bioinformatics* **29**, 1149–1157 (2013).
55. Cedar, H. & Bergman, Y. Linking DNA methylation and histone modification: patterns and paradigms. *Nat. Rev. Genet.* **10**, 295–304 (2009).
56. Humphries, L. A. et al. Pro-apoptotic TP53 homolog TAp63 is repressed via epigenetic silencing and B-cell receptor signalling in chronic lymphocytic leukaemia. *Br. J. Haematol.* **163**, 590–602 (2013).
57. Hildebrand, D. G. et al. IkappaBzeta is a transcriptional key regulator of CCL2/MCP-1. *J. Immunol.* **190**, 4812–4820 (2013).
58. Bolli, N. et al. Heterogeneity of genomic evolution and mutational profiles in multiple myeloma. *Nat. Commun.* **5**, 2997 (2014).
59. Lohr, J. G. et al Widespread genetic heterogeneity in multiple myeloma: implications for targeted therapy. *Cancer Cell* **25**, 91–101 (2014).
60. Walker, B. A. et al. Mutational spectrum, copy number changes, and outcome: results of a sequencing study of patients with newly diagnosed myeloma. *J. Clin. Oncol.* **33**, 3911–3920 (2015).
61. Totzke, G. et al. A novel member of the IkappaB family, human IkappaB-zeta, inhibits transactivation of p65 and its DNA binding. *J. Biol. Chem.* **281**, 12645–12654 (2006).
62. Wu, Z. et al. Nuclear protein IkappaB-zeta inhibits the activity of STAT3. *Biochem Biophys. Res Commun.* **387**, 348–352 (2009).
63. Derenne, S. et al. Antisense strategy shows that Mcl-1 rather than Bcl-2 or Bcl-x(L) is an essential survival protein of human myeloma cells. *Blood* **100**, 194–199 (2002).
64. Jourdan, M. et al. A major role for Mcl-1 antiapoptotic protein in the IL-6-induced survival of human myeloma cells. *Oncogene* **22**, 2950–2959 (2003).
65. Braggio, E. et al. Methylation status of nine tumor suppressor genes in multiple myeloma. *Int J. Hematol.* **91**, 87–96 (2010).
66. Mateos, M. V. et al. Methylation is an inactivating mechanism of the p16 gene in multiple myeloma associated with high plasma cell proliferation and short survival. *Br. J. Haematol.* **118**, 1034–1040 (2002).
67. Takada, S. et al. Methylation status of fragile histidine triad (FHIT) gene and its clinical impact on prognosis of patients with multiple myeloma. *Eur. J. Haematol.* **75**, 505–510 (2005).
68. Harris, M. E. et al. Regulation of histone mRNA in the unperturbed cell cycle: evidence suggesting control at two posttranscriptional steps. *Mol. Cell Biol.* **11**, 2416–2424 (1991).
69. Shaffer, A. L. et al. IRF4 addiction in multiple myeloma. *Nature* **454**, 226–231 (2008).
70. Iida, S. et al. Deregulation of MUM1/IRF4 by chromosomal translocation in multiple myeloma. *Nat. Genet.* **17**, 226–230 (1997).
71. Loven, J. et al. Selective inhibition of tumor oncogenes by disruption of super-enhancers. *Cell* **153**, 320–334 (2013).
72. Kronke, J. et al. Lenalidomide causes selective degradation of IKZF1 and IKZF3 in multiple myeloma cells. *Science* **343**, 301–305 (2014).
73. Lu, G. et al. The myeloma drug lenalidomide promotes the cereblon-dependent destruction of Ikaros proteins. *Science* **343**, 305–309 (2014).